

Magnetic-field dependence of energy levels in ultrasmall metal grains

S. Adam, M. L. Polianski, X. Waintal*, and P. W. Brouwer

Laboratory of Atomic and Solid State Physics, Cornell University, Ithaca, NY 14853-2501

March 22, 2022

We present a theory of mesoscopic fluctuations of g tensors and avoided crossing energies in a small metal grain. The model, based on random matrix theory, contains both the orbital and spin contributions to the g tensor. The two contributions can be experimentally separated for weak spin-orbit coupling while they merge in the strong coupling limit. For intermediate coupling, substantial correlations are found between g factors of neighboring levels.

PACS numbers: 71.70.Ej, 73.23.-b, 73.23.Hk

I. INTRODUCTION

Recent developments in nanofabrication techniques have allowed for the resolution of individual “particle-in-a-box” energy levels in small metal grains or semiconductor quantum dots using tunneling spectroscopy.^{1–4} In the absence of a magnetic field, the energy levels ε_μ are two-fold degenerate (Kramers’ degeneracy). An applied magnetic field B lifts the degeneracy; the splitting of the doublet is described with the help of a “ g factor”,

$$\delta\varepsilon_\mu = \mu_B g B, \quad (1)$$

where μ_B is the Bohr magneton. A cartoon of the magnetic-field dependence of the energy levels is shown in Fig. 1. Whereas $g = 2$ for electrons in vacuum, in a metal grain the g factor can be different from two as a result of spin-orbit scattering. Recently, the magnetic-field dependence of particle-in-a-box levels in metal grains have been measured by two groups.^{5–8} Measured g factors range from 0.1 to 2, depending on grain size, material, and, in the case of Ref. 5, doping with heavy ions.

Unlike in bulk metals, where g factors are used to describe the effect of spin-orbit coupling on the band structure, g factors in a metal grain are not a “bulk” property.⁹ Not only does the typical value of the g factors depend on the size of the metal grain, g factors also depend on the microscopic details such as the impurity configuration, the location of defects, and the form of the grain boundary. As a result, different energy levels in a metal grain have different g factors. Moreover, even if the metal grain is roughly spherical and without lattice anisotropy, the presence of impurities breaks the rotational symmetry on the microscopic scale, causing g factors to depend on the direction of the applied magnetic field. A statistical description of the level-to-level fluctuations of g factors in metal grains has been formulated by Matveev *et al.*¹⁰ and by Halperin and two of the authors¹¹ using random matrix theory (RMT). Petta and Ralph⁷ measured g factors for up to 9 consecutive levels in nanometer-size Cu, Ag, and Au grains and found good agreement with the distributions of Refs. 10,11. The dependence on the direction \hat{B} of the magnetic field is taken into account by replacing the g factor by a “ g tensor” \mathcal{G} ,¹²

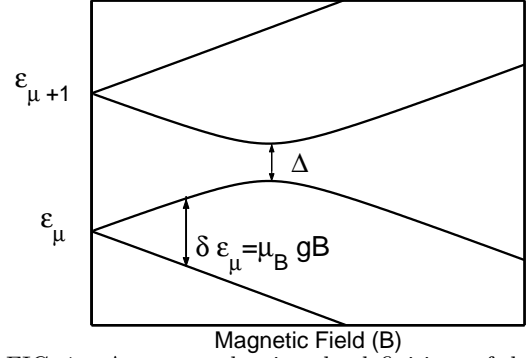


FIG. 1. A cartoon showing the definitions of the g -factors and the avoided crossing energy Δ . At zero magnetic field, all energy levels ε_μ are doubly degenerate. A magnetic field splits these doublets. The g -factor measures the size of the splitting of a doublet ε_μ as a function of magnetic field, see Eq. (1). The avoided crossing energy Δ is the minimum distance at the first avoided crossing of neighboring energy levels, see Sec. IV.

$$\delta\varepsilon_\mu = \mu_B B (\hat{B}^T \mathcal{G}_\mu \hat{B})^{1/2}. \quad (2)$$

(The g tensor carries a subscript μ to reflect its dependence on the energy level ε_μ .) The g -factor (1) for a magnetic field in the z direction is the square root of the tensor element \mathcal{G}_{zz} . A measurement of full g tensors in Cu grains was reported quite recently.⁸ Again, good agreement was found between the experimentally measured g -tensor distribution and RMT.

The effect of the spin-orbit interaction on the wavefunctions in a metal grain can be described by a dimensionless parameter λ ,

$$\lambda^2 = \frac{\pi \hbar}{\tau_{so} \delta}, \quad (3)$$

where τ_{so} is the spin-orbit scattering time and δ is the mean spacing between Kramers’ doublets in the grain (in the absence of the magnetic field). The effects of spin-orbit scattering are weak if $\lambda \ll 1$. In that case, wavefunctions are real and have a well-defined spin; the electron magnetic moment is close to its vacuum value $g = 2$. In the opposite limit of strong spin-orbit scattering, $\lambda \gg 1$, wavefunctions are complex and have no

well-defined spin. Hence, the spin contribution to the electron's magnetic moment is strongly suppressed, compared to the case of electrons in vacuum. However, in addition to a contribution from the electron's spin, there may be a significant orbital contribution to the magnetic moment carried by a single electron if spin-orbit scattering is present: wavefunctions are complex, and hence current-carrying.¹⁰

Experimental estimates of λ are close to zero in Al and range from 0.7 in a small Cu grain ($\delta \approx 0.7$ meV) to 13 in a larger Au grain ($\delta \approx 0.1$ meV).⁷ A full theory of the combined orbital and spin contributions to the g tensor was developed for the asymptotes $\lambda \ll 1$ and $\lambda \gg 1$ only.^{10,11} Both theories calculate distributions normalized to the average $(\langle g^2 \rangle)^{1/2}$. In addition, Matveev *et al.* calculate both spin and orbital contributions to $(\langle g^2 \rangle)^{1/2}$, while Ref. 11 considered the spin contribution only. The case of intermediate λ , necessary for a quantitative comparison with the experiments of Ref. 7, was studied in Ref. 11 using numerical diagonalization of a random matrix model with variable spin-orbit scattering strength, but without inclusion of the orbital contribution to the magnetization.

In this paper we construct a random matrix theory that describes both spin and orbital contributions to the electron g tensor. In the limit $\lambda \gg 1$ our model reproduces the g tensor distribution found in Refs. 10,11, but it also provides a simple model to numerically obtain the full g tensor distribution for arbitrary spin-orbit scattering strength. In addition to the distribution of the g tensor we also look at the correlator of g tensors of neighboring levels. While g tensors are not correlated for $\lambda = 0$ and, as we show here, for $\lambda \gg 1$; we find that correlations can be substantial for λ of order unity. The random-matrix model is formulated in Sec. II; the g tensor distributions are considered in Sec. III.

In addition to the g factors, which describe the magnetic-field dependence of the energy levels at very small magnetic fields, Salinas *et al.* obtained additional information on the magnitudes of spin-orbit scattering matrix elements from avoided crossings of energy levels at higher magnetic fields: For weak spin-orbit scattering, the minimal energy separation Δ in an avoided crossing between the downward moving level $\varepsilon_{\mu+1,-}$ and the upward moving level $\varepsilon_{\mu,+}$ is twice the matrix element of the spin-orbit coupling between the corresponding eigenstates,⁵ see Fig. 1. In Sec. IV we calculate the avoided crossing energy Δ from the random matrix model, and find its statistical distribution and dependence on the direction of the magnetic field \vec{B} .

II. RANDOM MATRIX MODEL

In this section we formulate a random-matrix model that describes the magnetic-field dependence of energy levels in a metal grain with spin-orbit scattering, taking

into account both the Zeeman and the orbital effects of the magnetic field. Following the basic premises of random matrix theory, we replace the Hamiltonian of the metal grain by a $2N \times 2N$ matrix \mathcal{H} ,

$$\mathcal{H}(\lambda) = H_{\text{GOE}} + \frac{\lambda}{\sqrt{N}} H_{\text{GSE}} + H_B. \quad (4)$$

The first two terms on the right hand side of Eq. (4) describe the Hamiltonian in the absence of the magnetic field; the last term H_B describes the effect of the magnetic field. Without the magnetic field, \mathcal{H} is taken from an ensemble that interpolates between the Gaussian Orthogonal and Gaussian Symplectic ensembles of random matrix theory. The Gaussian Orthogonal Ensemble (GOE), which is relevant for metal grains without spin-orbit scattering, consists of real symmetric $N \times N$ matrices with independently and Gaussian distributed elements, multiplied by the 2×2 unit matrix $\mathbb{1}_2$ in spin space,

$$H_{\text{GOE}} = S \otimes \mathbb{1}_2, \quad P(S) \propto e^{-(\pi^2/4N\delta^2)\text{tr } S^T S}. \quad (5)$$

Here δ is the mean level spacing in the metal grain (i.e., the mean spacing of the Kramers' doublets). The Gaussian Symplectic Ensemble (GSE), which describes metal grains with strong spin-orbit scattering, consists of self-dual quaternion matrices.¹⁴ A Hamiltonian taken from the GSE can be parameterized as

$$H_{\text{GSE}} = \frac{1}{2} \left(A_0 \otimes \mathbb{1}_2 + i \sum_{j=1}^3 A_j \otimes \sigma_j \right), \quad (6)$$

where A_0 is a real symmetric $N \times N$ matrix and the A_j , $j = 1, 2, 3$, are real and antisymmetric $N \times N$ matrices. The four matrices A_0 , A_1 , A_2 , and A_3 have independently and Gaussian distributed elements,

$$P(A_j) \propto e^{-(\pi^2/4N\delta^2)\text{tr } A_j^T A_j}, \quad j = 0, 1, 2, 3. \quad (7)$$

The crossover parameter λ describes the strength of the spin-orbit scattering in the Hamiltonian of Eq. (4). The cases $\lambda = 0$ and $\lambda \rightarrow \infty$ correspond to the GOE and GSE, respectively.

The effect of the magnetic field $\vec{B} = (B_1, B_2, B_3)$ is described by the term H_B in Eq. (4),

$$H_B = \sum_{j=1}^3 B_j M_j, \quad (8)$$

where the $2N \times 2N$ matrices M_j ($j = 1, 2, 3$) are given by

$$M_j = \mu_B \left(\mathbb{1}_N \otimes \sigma_j + i \frac{\pi\eta}{\delta\sqrt{N}} X_j \otimes \mathbb{1}_2 \right), \quad (9)$$

where the X_j , $j = 1, 2, 3$, are real antisymmetric matrices, with independent and Gaussian distributions,

$$P(X_j) \propto e^{-(\pi^2/4N\delta^2)\text{tr } X_j^T X_j}. \quad (10)$$

The first term in Eq. (9) describes the coupling of the magnetic field to the electron spin; the second term, which is diagonal in spin space, describes the coupling of the magnetic field to the orbital angular momentum. The second term in Eq. (9) was originally proposed by Pandey and Mehta to describe the orbital effect of a time-reversal symmetry breaking magnetic field on the statistics of energy levels.^{13,16} For a diffusive spherical grain with radius R , mean free path l , and effective electron mass m^* , the coefficient η is given by¹⁷

$$\eta^2 = (m/m^*)^2 \frac{l}{5R}, \quad (11)$$

whereas for a ballistic sphere with diffuse boundary scattering, one has¹⁸

$$\eta^2 = (m/m^*)^2 \frac{1}{8}. \quad (12)$$

At the end of the calculation, the limit $N \rightarrow \infty$ is taken. Without the orbital term, the Hamiltonian \mathcal{H} of Eq. (4) is the same as the random-matrix Hamiltonian used by Halperin and two of the authors in Ref. 11.

The g tensor \mathcal{G} and the avoided crossing energy Δ will be expressed in terms of matrix elements involving the eigenvectors of the Hamiltonian (4). Eigenvectors ψ_μ of the Hamiltonian (4) are $2N$ component complex vectors. Their elements are denoted as $\psi_\mu(n, \sigma)$, where $n = 1, \dots, N$ refers to the “orbital” degrees of freedom, and $\sigma = \pm 1$ to spin. At zero magnetic field, all eigenvalues of the Hamiltonian (4) are twofold degenerate (Kramers’ degeneracy): each eigenvalue ε_μ ($\mu = 1, \dots, N$) has two orthogonal eigenvectors ψ_μ and $\mathcal{T}\psi_\mu$ where $\mathcal{T}\psi(n, \sigma) = \sigma\psi^*(n, -\sigma)$, is the time-reversed of ψ . In the GOE ($\lambda = 0, B = 0$), the eigenvectors ψ_μ and $\mathcal{T}\psi_\mu$ can be chosen such that $\psi_\mu(n, +1) = -\mathcal{T}\psi_\mu(n, -1)$ is a real number and $\psi_\mu(n, -1) = \mathcal{T}\psi_\mu(n, 1) = 0$. In that case, the nonzero elements $\psi_\mu(n, +1)$ are independently and Gaussian distributed with zero mean and with variance $1/N$.¹⁴ (Of course, any linear combination of ψ_μ and $\mathcal{T}\psi_\mu$ forms a valid pair of eigenvectors for the eigenvalue ε_μ as well.) In the GSE ($\lambda \rightarrow \infty, B = 0$), the elements of ψ_μ are complex numbers with independent and Gaussian distributions with variance $1/2N$. In both the GSE and the GOE different eigenvectors are statistically uncorrelated.

In the crossover between GOE and GSE, the eigenvector distribution is more complicated than in each of the two basic ensembles. Unlike for the cases of the pure GOE and GSE, eigenvectors at different energy levels are correlated, so that it is no longer sufficient to look at the distribution of one eigenvector alone.¹⁵ Since orthogonal invariance is preserved throughout the GOE-GSE crossover, the problem of finding the (joint) distribution of one or more eigenvectors in the crossover ensemble can be simplified by considering their orthogonal invariants

first. For each pair of eigenstates ψ_μ and ψ_ν , the invariants are four quaternion numbers $\rho_{\mu\nu}^j$, $j = 0, 1, 2, 3$. If we diagonalize \mathcal{H} , writing

$$\mathcal{H}(B = 0) = U(E \otimes \mathbb{1}_2)U^\dagger, \quad (13)$$

where U is the symplectic eigenvector matrix and the $N \times N$ diagonal matrix E contains the eigenvalues ε_μ on the diagonal, they are

$$\begin{aligned} \rho_{\mu\nu}^0 &= [U^\dagger U]_{\mu\nu} \\ &= \delta_{\mu\nu} \mathbb{1}_2 \end{aligned} \quad (14)$$

$$\begin{aligned} \rho_{\mu\nu}^j &= i[U^\dagger \sigma_j U]_{\mu\nu} \\ &= \begin{pmatrix} (\rho_{\mu\nu}^j)_{++} & (\rho_{\mu\nu}^j)_{+-} \\ (\rho_{\mu\nu}^j)_{-+} & (\rho_{\mu\nu}^j)_{--} \end{pmatrix}, \quad j = 1, 2, 3. \end{aligned} \quad (15)$$

The $\rho_{\mu\nu}^j$ satisfy a criterion of anti-hermiticity,

$$\rho_{\mu\nu}^j = -(\rho_{\nu\mu}^j)^\dagger, \quad j = 1, 2, 3. \quad (16)$$

The orthogonal invariants $\rho_{\mu\nu}^0$ express orthonormality of the eigenvectors ψ_μ and $\mathcal{T}\psi_\mu$. The remaining orthogonal invariants $\rho_{\mu\nu}^j$ are characteristic for the crossover and determine to what extent spin-rotation symmetry has been broken. In the GOE, we have: $\sum_k \text{tr}(\rho_{\mu\mu}^i \sigma_k) \text{tr}(\rho_{\mu\mu}^j \sigma_k) = 4\delta_{ij}$, while $\rho_{\mu\nu}^j = 0$ if $\mu \neq \nu$; in the GSE, $\rho_{\mu\nu}^j = 0$ for all μ and ν . An average involving different eigenvectors is then calculated in two steps: First, eigenvector elements have a Gaussian distribution with zero mean and with variance determined by the orthogonal invariants.¹⁵ In spinor notation, where $\psi(n)$ denotes the 2-component spinor with elements $\psi(n, +1)$ and $\psi(n, -1)$, these variances are

$$\begin{aligned} \langle \psi_\mu(n)^\dagger \psi_\nu(m) \rangle &= \frac{\delta_{mn}}{N} \delta_{\mu\nu}, \\ i \langle \psi_\mu(n)^\dagger \sigma_j \psi_\nu(m) \rangle &= \frac{\delta_{mn}}{N} (\rho_{\mu\nu}^j)_{++}, \\ \langle \psi_\mu(n)^T \sigma_2 \psi_\nu(n) \rangle &= 0, \\ \langle \psi_\mu(n)^T \sigma_2 \sigma_j \psi_\nu(n) \rangle &= \frac{\delta_{mn}}{N} (\rho_{\mu\nu}^j)_{-+}. \end{aligned} \quad (17)$$

With the help of Eq. (17) any average over eigenvectors can be expressed in terms of the orthogonal invariants involved in the problem.

What remains is to find the average over a small number of orthogonal invariants. To our knowledge, a solution of this problem exists for the limits $\lambda \ll 1$ and $\lambda \gg 1$ only. For strong spin-orbit scattering, $\lambda \gg 1$, the solution takes the form of a surmise equating the distribution of the $\rho_{\mu\nu}^j$ for the $2N \times 2N$ crossover Hamiltonian (4) to the distribution of the same quantities for a GSE Hamiltonian of a smaller size $2N'$,¹⁵

$$\begin{aligned} N' &= \lambda^2 N (\lambda^2 + 2N) / (\lambda^2 + N)^2 \\ &\rightarrow 2\lambda^2 \quad \text{if } N \rightarrow \infty, \end{aligned} \quad (18)$$

provided the energy difference $|\varepsilon_\mu - \varepsilon_\nu| \ll \lambda^2 \delta$. This means that the elements of the matrix ρ^j are uncorrelated and that they have a Gaussian distribution with variance

$$\begin{aligned} \langle |(\rho_{\mu\nu}^j)_{++}|^2 \rangle &= \frac{1}{2N}, \\ \langle |(\rho_{\mu\nu}^j)_{+-}|^2 \rangle &= \frac{1 + \delta_{\mu\nu}}{2N}. \end{aligned} \quad (19)$$

A similar surmise was proposed in Ref. 15 for the eigenvector statistics in the crossover between the GOE and the Gaussian Unitary Ensemble of random-matrix theory. The motivation of this surmise becomes clear once we consider the crossover Hamiltonian (4) in the eigenvector basis of H_{GOE} .¹⁵ In this basis, eigenvectors of the crossover Hamiltonian are “localized”: they are mainly built up from eigenvectors of H_{GOE} with energies inside a window of size $\sim N'\delta$ (with N' to be determined later). Since changing to the GOE basis does not change orthogonal invariants, we can calculate the $\rho_{\mu\nu}^j$ using an effective $2N' \times 2N'$ Hamiltonian that contains the $2N'$ relevant GOE eigenvectors only, if $|\mu - \nu| \ll N'$. As the spin-rotational symmetry breaking term is large for the effective Hamiltonian, its distribution is that of the GSE, not a crossover. The exact relation (18) between N' and N is found matching the distributions of a single orthogonal invariant $\rho_{\mu\mu}^j$ in the crossover Hamiltonian and in the GSE.¹¹

In the following two sections, the random matrix model (4) will serve as a starting point for analytical calculations of the g tensor distribution and avoided crossing energies in the regimes of weak spin-orbit scattering, $\lambda \ll 1$, and of strong spin orbit scattering, $\lambda \gg 1$, and for numerical calculations of the g -tensor distribution in the crossover regime $\lambda \approx 1$. The case of weak spin-orbit scattering can be treated using perturbation theory in λ ; for strong spin-orbit scattering, we use the full eigenvector distribution of the GOE-GSE crossover Hamiltonian and the surmise for the orthogonal invariants that was discussed in this section.

III. STATISTICS OF THE G TENSOR

A typical plot of the magnetic field dependence of energy levels is shown in Fig. 1. A magnetic field $\vec{B} = B\hat{B}$ splits the Kramers' doublets ε_μ into pairs $\varepsilon_{\mu,\pm}$ that depend linearly on the magnitude B of the magnetic field,

$$\varepsilon_{\mu,\pm} = \varepsilon_\mu \pm \frac{1}{2}\delta\varepsilon_\mu, \quad (20)$$

with $\delta\varepsilon_\mu$ expressed in terms of the g tensor \mathcal{G}_μ as in Eq. (2) above. Following Ref. 11, the g tensor can be written as

$$\mathcal{G} = G^T G, \quad (21a)$$

where the 3×3 matrix G has elements

$$\begin{aligned} G_{1j} &= \frac{2}{\mu_B} \text{Re} \langle \psi_\mu | M_j | \mathcal{T} \psi_\mu \rangle, \\ G_{2j} &= \frac{2}{\mu_B} \text{Im} \langle \psi_\mu | M_j | \mathcal{T} \psi_\mu \rangle, \\ G_{3j} &= \frac{2}{\mu_B} \langle \psi_\mu | M_j | \psi_\mu \rangle, \end{aligned} \quad (21b)$$

where M_j is defined in Eq. (9), ψ_μ is an eigenvector of \mathcal{H} at $B = 0$ with eigenvalue ε_μ , and $\mathcal{T}\psi_\mu$ is its time-reversed.

The tensor \mathcal{G} has three eigenvectors and three eigenvalues g_j^2 , $j = 1, 2, 3$. The eigenvectors are referred to as “principal axes”, the eigenvalues g_1 , g_2 , and g_3 as “principal g -factors”. The three principal g factors describe the splittings of the doublet for magnetic fields along each of the three principal axes. We describe the distribution of the g tensor in terms of the distributions of its eigenvectors (the principal axes) and eigenvalues (the principal g -factors). For a roughly spherical grain, the principal axes will be oriented randomly in space. Hence, it remains to find the distribution of the three principal g factors $g_{\mu,1}$, $g_{\mu,2}$, and $g_{\mu,3}$. We will now consider the cases of weak and strong spin-orbit scattering separately.

A. Weak spin-orbit scattering

To leading order in $\lambda \ll 1$, $\eta\lambda \ll 1$ the g tensor reads

$$\begin{aligned} \mathcal{G}_{\mu;ij} &= 4 \left(\delta_{ij} + \frac{\eta\lambda\pi}{N\delta} \sum_{\nu \neq \mu} \frac{X_i^{\mu\nu} A_j^{\mu\nu} + A_i^{\mu\nu} X_j^{\mu\nu}}{\varepsilon_\mu - \varepsilon_\nu} \right. \\ &\quad \left. - \frac{\lambda^2}{N} \sum_{\nu \neq \mu} \frac{\delta_{ij} \sum_{k=1}^3 (A_k^{\mu\nu})^2 - A_i^{\mu\nu} A_j^{\mu\nu}}{(\varepsilon_\mu - \varepsilon_\nu)^2} \right). \end{aligned} \quad (22)$$

Here ε_μ and ε_ν are eigenvalues of the Hamiltonian (4) at zero magnetic field and without spin-orbit scattering, and $A_j^{\mu\nu}$ and $X_j^{\mu\nu}$ are the matrix element of the matrices A_j and X_j between the corresponding eigenvectors $|\psi_\mu\rangle$ and $|\psi_\nu\rangle$ of \mathcal{H} , respectively, cf. Eqs. (6) and (9). In Eq. (22) we neglected terms of order $\lambda^2\eta$, $(\lambda\eta)^2$, which are small compared to $\lambda\eta$, and of third (and higher) order in λ . The second term in Eq. (22) corresponds to orbital paramagnetism, and is of order $\eta\lambda$ because the orbital contribution couples to complex wavefunctions that occur for $\lambda \neq 0$. The λ^2 term is a reduction of the Pauli paramagnetism caused by interaction with other energy levels and for the case of $i = j = 3$, agrees with earlier work.¹⁹

The distribution of \mathcal{G} without the orbital contribution (second term in Eq. (22)) was studied in Refs. 10 and 11. For very small spin-orbit scattering, however, the orbital part is found to dominate the g tensor fluctuations, since it is of first order in the spin-orbit scattering strength λ , while the Zeeman contribution is of order λ^2 . Whereas the Zeeman contribution always gives g factors smaller

than two — the last term in Eq. (22) is negative definite — the orbital contribution can be of arbitrary sign, allowing for principal g factors larger than two. To illustrate this feature, we calculate the tails of the joint distribution $P(g_1, g_2, g_3)$ of the three principal g factors. The distribution of the tails is dominated by events where the spacing between the level ε_μ and one of its neighbors $\varepsilon_{\mu+1}$ or $\varepsilon_{\mu-1}$ is exceptionally small, of order $\lambda\delta$ or $\lambda\eta\delta$ (whichever is larger). Hence, the tails of $P(g_1, g_2, g_3)$ can be calculated limiting attention to the nearest-neighbor terms in the summations in Eq. (22). We order the three principal g factors as $g_1 < g_2 < g_3$ and parameterize them as $g_j = 2(1 + y_j)$, $j = 1, 2, 3$. Hence, the tails of the distribution correspond $|y_j| \gg \max(\lambda^2, \lambda\eta)$ for at least one of the y_j . With the definition $\Theta(x) = 1$ for $x > 0$, and $\Theta(x) = 0$ for $x < 0$, the tails of the distribution are found to be

$$P(y_1 < y_2 < y_3) = \frac{3(\pi\lambda)^2}{8\eta^3} \Theta(-y_2) \times \frac{y_3 - y_1}{(-\pi y_2)^{7/2}} \exp \left[\frac{(y_1 - y_2 - y_3)^2 + 4(y_1 - y_2)y_2}{4\eta^2 y_2} \right]. \quad (23)$$

In the limit $\eta \ll \lambda$ the tail of the distribution factors as

$$P(y_1 < y_2 < y_3) \propto \frac{y_3 - y_1}{\eta^3 (-y_2)^{7/2}} \exp \left[\frac{y_1 - y_2}{\eta^2} + \frac{y_3^2}{4\eta^2 y_2} \right],$$

reproducing the result

$$P = \frac{3\lambda^2}{4\pi y_2^2} \delta(y_3) \delta(y_2 - y_1) \quad (24)$$

for the tail of the g tensor distribution obtained in Ref. 11 in the limit $\eta \rightarrow 0$. In the opposite limit $\lambda \ll \eta$, Eq. (23) simplifies to

$$P(y_1, y_2, y_3) = \frac{9\eta^2 \lambda^2 \Theta(-y_1) \delta(y_2) \Theta(y_3)}{\pi (y_1 - y_3)^4}. \quad (25)$$

Equation (24) is valid if $|y_1|, |y_2| \gg \lambda^2$; Eq. (25) holds if $|y_1|, |y_3| \gg \lambda\eta$.

In Fig. 2 we have shown the distributions of the principal g factors g_1 , g_2 , and g_3 , calculated from the random matrix model (4) using numerical diagonalization. Although the limits (24) and (25) were derived for the tail of the g -tensor distribution only, they can account for some qualitative features of the full g -tensor distribution for weak spin-orbit scattering shown in Fig. 2: when the orbital contribution to the g tensor dominates ($\eta \gg \lambda$), generically $g_3 > 2$, $g_2 \approx 2$, and $g_1 < 2$, cf. Eq. (25). On the other hand, when the Zeeman contribution to the g tensor dominates ($\eta \ll \lambda$), one typically has $g_1 \approx g_2 < 2$ and $g_3 \approx 2$, cf. Eq. (24).

We now turn our attention to correlations between g tensors of neighboring levels. Such correlations are described by the correlator

$$\mathcal{C}_{ij,kl} = \langle g_\mu^2 \rangle^{-2} (\langle \mathcal{G}_{\mu,ij} \mathcal{G}_{\mu+1,kl} \rangle - \langle \mathcal{G}_{\mu,ij} \rangle \langle \mathcal{G}_{\mu+1,kl} \rangle). \quad (26)$$

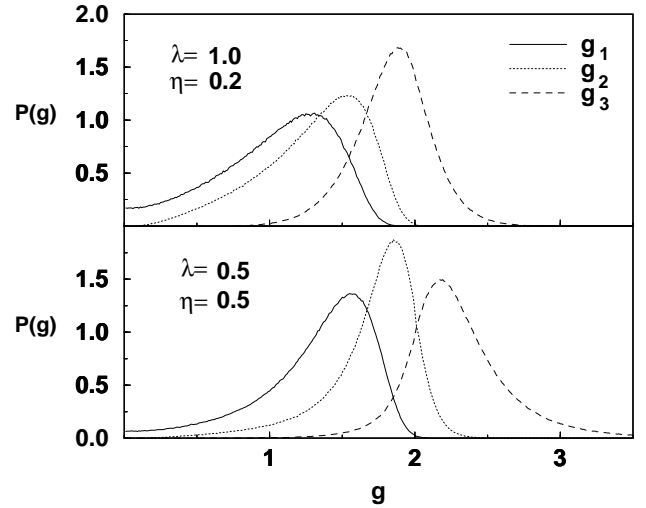


FIG. 2. Distributions of magnitudes of the principal g factors. Upper panel: $\lambda = 1.0$, $\eta = 0.2$; Lower panel: $\lambda = \eta = 0.5$.

Calculating the correlator \mathcal{C} to leading order in $\lambda \ll 1$, we find that the result is dominated by events where the levels ε_μ and $\varepsilon_{\mu+1}$ are very close. Since this contribution is formally divergent, as a result of the presence of the energy denominators in the perturbation expression (22), a cut off must be imposed at energy separations $\varepsilon_{\mu+1} - \varepsilon_\mu$ of order $\lambda\delta$ where the perturbation theory is not valid. To treat the contribution from nearby levels $\varepsilon_{\mu+1}$ and ε_μ correctly, we calculate the contribution from such events non-perturbatively. To leading order in $\lambda \ll 1$, the result of such a treatment amounts to the replacement of the energy denominator $\varepsilon_{\mu+1} - \varepsilon_\mu$ in Eq. (22) by $[(\varepsilon_{\mu+1} - \varepsilon_\mu)^2 + |\vec{A}|^2 \lambda^2 / N]^{1/2}$, where \vec{A} is shorthand notation for the vector with components $A_j^{\mu, \mu+1}$, $j = 1, 2, 3$. We then obtain the following result:

$$\mathcal{C}_{ijkl} = \frac{\lambda^2}{\pi} (\delta_{ik} \delta_{jl} + \delta_{il} \delta_{jk}) (\eta^2 \ln \lambda + \frac{1}{20}) + \frac{3\lambda^2}{10\pi} \delta_{ij} \delta_{kl}. \quad (27)$$

The correlator between g factors (at a fixed direction of the magnetic field) is found from Eq. (27) setting $i = j = k = l = \hat{B}$ in the direction of magnetic field,

$$\mathcal{C} = \langle g_{\mu+1}^2 g_\mu^2 \rangle / \langle g^2 \rangle^2 - 1 = \frac{2\lambda^2}{\pi} \left(\eta^2 \ln \lambda + \frac{1}{5} \right). \quad (28)$$

B. Strong spin-orbit scattering

In the regime of a strong spin-orbit scattering, $\lambda \gg 1$, the g tensor distribution can be calculated from Eq. (21) using the known distribution of the eigenvectors of the random Hamiltonian (4) at zero magnetic field, see Sec.

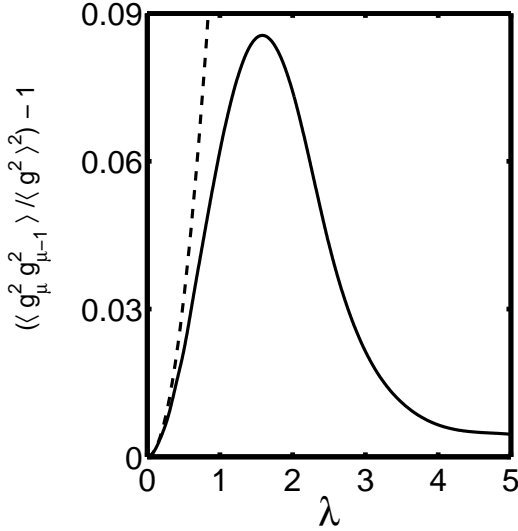


FIG. 3. g -factor correlation as a function of spin-orbit coupling λ computed numerically for 200×200 GOE-GSE crossover matrices. Dashed line shows the result from perturbation theory Eq. (28).

II. We then find that the matrix elements of the 3×3 matrix G of Eq. (21) are Gaussian random numbers, with zero mean and with variance $1/\lambda^2 + 2\eta^2$. From this we conclude that the distribution of the principal g factors is¹¹

$$P(g_1, g_2, g_3) \propto \left(\prod_{i < j} |g_i^2 - g_j^2| \right) \prod_i e^{-3g_i^2/2\langle g^2 \rangle}, \quad (29)$$

where

$$\langle g^2 \rangle = \frac{1}{3} \langle g_1^2 + g_2^2 + g_3^2 \rangle = \frac{3}{\lambda^2} + 6\eta^2. \quad (30)$$

Values for η for diffusive and ballistic spherical grains are given in Eqs. (11) and (12). Equations (29) and (30) extend the result of Ref. 11 to the case $\eta \neq 0$. Equation (30), which was derived using the random matrix model (4), agrees with the results of Matveev *et al.*, which were derived using a comparison of the g factors and the energy absorption of a time-dependent magnetic field.

In Fig. 4 we show the result of numerical calculations of $\langle g^2 \rangle$ as a function of the spin-orbit scattering rate λ and for various values of η . For $\eta^2 < 2/3$, $\langle g^2 \rangle < 2$ for all λ , while for $\eta^2 > 2/3$, $\langle g^2 \rangle > 2$. The derivatives with λ are maximal near $\lambda = 0$ because of the enhanced fluctuations due to the orbital part at small λ , cf. Eq. (22).

Correlations between g tensors of neighboring levels trivially vanish for large λ because, in the GSE, different eigenvectors are statistically uncorrelated. However, since the average g tensor also depends on λ , it is a more meaningful question to study the correlator between g tensors, normalized by the average g factor, cf. Eq. (26). In the presence of an orbital contribution to the g tensor, the average g factors are nonzero for $\lambda \gg 1$, see Eq. (30),

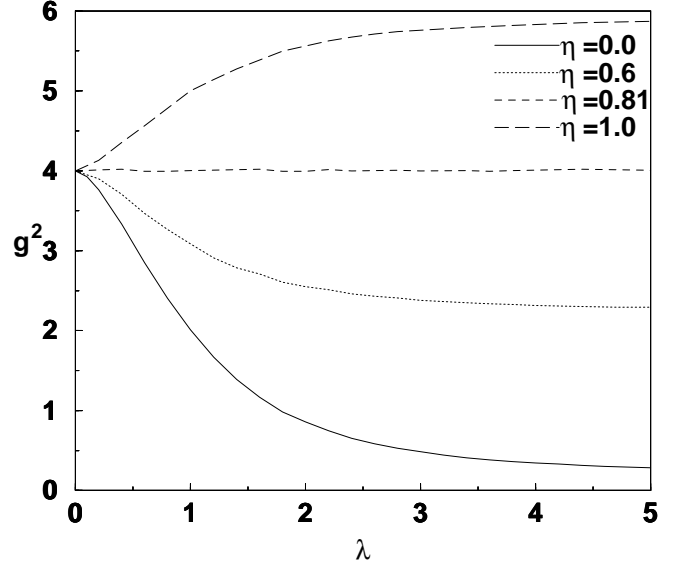


FIG. 4. Averaged $\langle g^2 \rangle$ as a function of spin-orbit strength λ . The critical value $\eta_0 = \sqrt{2/3} \approx 0.81$.

so that the vanishing of correlations in the GSE implies that they vanish compared to the average as well. Without the orbital contribution, g -tensor correlations cannot be addressed with reference to the eigenvector statistics in the GSE, because $\mathcal{G} = 0$ in the GSE. Instead we need the more detailed knowledge of the eigenvector distribution for large λ , which is summarized in Sec. II. The main result of that section is that the eigenvector distribution depends on the distribution of certain orthogonal invariants $\rho_{\mu\nu}^j$, $j = 1, 2, 3$ which are 2×2 matrices in spin space, see. Eq. (17). With the help of Eq. (21), one easily verifies that, in the case $\eta = 0$, the g tensor may be expressed in terms of these orthogonal invariants only,

$$(\mathcal{G}_\mu)_{ij} = 2\text{tr} \rho_{\mu\mu}^i \rho_{\mu\mu}^j, \quad i, j = 1, 2, 3, \quad (31)$$

where the trace is taken in spin space. Since, for $\lambda \gg 1$, the orthogonal invariants $\rho_{\mu\mu}^j$ are all independently distributed for different levels, we conclude that g tensors of different levels are uncorrelated in the case $\eta = 0$ as well.

Figure 3 shows the g -factor correlator (28) normalized by the average g factor as a function of λ . The numerical diagonalization confirms our previous conclusions that g factor correlations are small for both asymptotic regimes $\lambda \ll 1$ and $\lambda \gg 1$. Correlations are maximal for intermediate spin-orbit scattering strengths, $\lambda \sim 1.5$, but never amount to more than 10% of the average $\langle g^2 \rangle$.

IV. AVOIDED CROSSING ENERGIES

Once the Kramers' doublets are split by the magnetic field, half of the levels move upward with slope

$\sim (1/2)g\mu_B B$, while the other half moves downward with the same slope. Hence, a downward moving level $\varepsilon_{\mu+1,-}$ and the upward moving level $\varepsilon_{\mu,+}$ meet at magnetic field strength

$$B_c = \frac{2(\varepsilon_{\mu+1} - \varepsilon_{\mu})}{\mu_B(g_{\mu} + g_{\mu+1})}. \quad (32)$$

In fact, since the matrix element of the coupling H_B to the magnetic field between the corresponding eigenstates $|\psi_{\mu+1,-}\rangle$ and $|\psi_{\mu,+}\rangle$ is finite, the two levels do not cross, but exhibit an avoided crossing, see Fig. 1. In this section we calculate the minimum distance Δ between the energy levels in the avoided crossing, its dependence on the direction \hat{B} of the magnetic field, and its level-to-level fluctuations.

The avoided crossing energy is well-defined only if the magnetic field dependence of the two levels $\varepsilon_{\mu+1,-}(B)$ and $\varepsilon_{\mu,+}(B)$ is linear, the only exception being the curvature resulting from their mutual interaction at the avoided crossing. For the magnetic field strengths of interest, $B \sim B_c$, other sources of level curvature as a function of the magnetic field, which arise both from the spin and orbital couplings in the Hamiltonian H_B of Eq. (8), are small if both $\lambda \ll 1$ and $\eta \ll 1$. Hence, for the purpose of calculating the avoided crossing energy Δ it is sufficient to consider the perturbative regime of small λ and small η .

Considering the Hamiltonian in the basis of states $|\psi_{\mu+1,-}\rangle$ and $|\psi_{\mu,+}\rangle$, corresponding to the energy levels $\varepsilon_{\mu+1,-}$ and $\varepsilon_{\mu,+}$ at zero magnetic field, respectively,

$$\mathcal{H} = \begin{pmatrix} \varepsilon_{\mu+1} - \frac{1}{2}\mu_B B g_{\mu} & \langle \psi_{\mu+1,-} | \mathcal{H}_B | \psi_{\mu,+} \rangle \\ \langle \psi_{\mu,+} | \mathcal{H}_B | \psi_{\mu+1,-} \rangle & \varepsilon_{\mu} + \frac{1}{2}\mu_B B g_{\mu-1} \end{pmatrix}, \quad (33)$$

we find that the avoided crossing energy Δ reads

$$\begin{aligned} \Delta &= 2|\langle \psi_{\mu+1,-} | \mathcal{H}_{B_c} | \psi_{\mu,+} \rangle| \\ &= \frac{4|\varepsilon_{\mu+1} - \varepsilon_{\mu}|}{\mu_B(g_{\mu+1} + g_{\mu})} |\langle \psi_{\mu+1,-} | \hat{B} \cdot \vec{M} | \psi_{\mu,+} \rangle|. \end{aligned} \quad (34)$$

Using first order perturbation theory in λ and η , we find

$$\Delta = \lambda \left| \hat{B} \times \left(\frac{1}{\sqrt{N}} \vec{A}^{\mu+1,\mu} \right) \right|, \quad (35)$$

plus terms of order $\lambda\eta$ which are not relevant in the regime we consider. The components of the vector $\vec{A}^{\mu+1,\mu}$ are matrix elements of the spin-orbit matrices A_j , $j = 1, 2, 3$ of Eq. (6) in the basis that diagonalizes the Hamiltonian to zeroth order in λ .

In order to find the distribution of the avoided crossing energy Δ , we write

$$\Delta = \Delta_0 \sin \theta, \quad (36)$$

where $0 \leq \theta \leq \pi$ is the angle between the direction \hat{B} of the applied magnetic field and the vector $\vec{A}^{\mu+1,\mu}$. Using

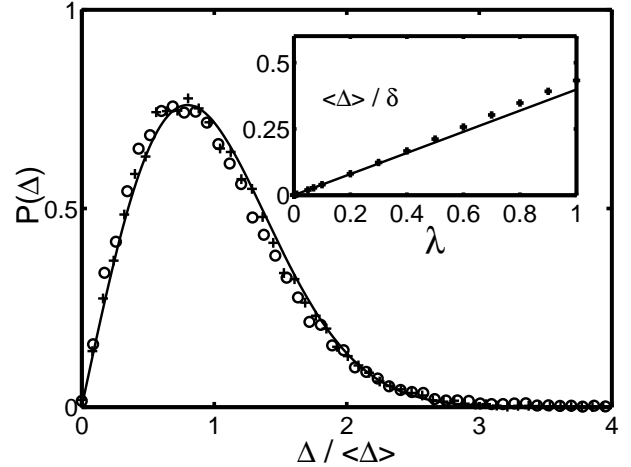


FIG. 5. Main panel: Distribution of the avoided crossing energy Δ . Solid line is the perturbative result (39); the data points are from numerical evaluation of Eq. (34) using the numerical diagonalization of the random matrix model (4) with $\eta = 0$ and $\lambda = 0.2$ (crosses), and $\lambda = 0.4$ (circles). Inset: Comparison of perturbation theory (solid curve) and numerical results (data points) for the average $\langle \Delta \rangle$.

the known distribution (7) of the spin-orbit coupling matrices A_j ($j = 1, 2, 3$), one finds that the three elements of $\vec{A}^{\mu+1,\mu}$ each have a Gaussian distribution with zero mean and with variance $N\delta^2/\pi^2$. Hence, we conclude that the vector $\vec{A}^{\mu+1,\mu}$ is randomly oriented in space, so that

$$P(\theta) = \frac{1}{2} \sin \theta, \quad (37)$$

and that

$$P(\Delta_0) = \frac{(\Delta_0 \pi)^2 \sqrt{2\pi}}{(\lambda \delta)^3} \exp \left[-\frac{1}{2} \left(\frac{\pi \Delta_0}{\lambda \delta} \right)^2 \right]. \quad (38)$$

Equations (36)–(38) not only give the full distribution of the avoided crossing energy Δ , but also the dependence of Δ on the direction \hat{B} of the magnetic field. Equations (36)–(38) can be combined to give

$$P(\Delta) = \frac{\pi^2 \Delta}{(\lambda \delta)^2} \exp \left[-\frac{1}{2} \left(\frac{\pi \Delta}{\lambda \delta} \right)^2 \right]. \quad (39)$$

The latter result is relevant for comparison with experiments where the direction of the magnetic field cannot be varied.^{5,7}

Figure 5 shows the distribution (39), together with results from a numerical calculation of the distribution of Eq. (34) using the random matrix model (4) for $\eta = 0$ and two different values of λ . We see that the agreement between the numerical diagonalization of the random matrix model and the distribution (39) calculated using first order perturbation theory in λ remains good up to $\lambda \sim 1$.

[We should note, however, that the approximations leading to an avoided crossing energy that is dominated by matrix elements involving two neighboring levels only, is valid for $\lambda \ll 1$ and $\eta \ll 1$ only, see the discussion preceding Eq. (34).] Although there are corrections to $P(\Delta)$ to second order in λ , the first nonzero corrections to the average $\langle \Delta \rangle$ appear to third order in λ only.

V. DISCUSSION AND CONCLUSIONS

In this paper, we have presented a random matrix theory for the distributions of g tensors and avoided crossing energies in small metal grains with spin-orbit scattering. Our theory includes both the spin and the orbital effects of the magnetic field.

For large spin-orbit scattering, the main effect of the orbital contribution is to increase the typical size of the g tensor; the fluctuations (normalized by the average) and the relative magnitudes of the three principal g values are the same with and without a large orbital contribution.¹¹ For weak spin-orbit scattering, the presence of an orbital contribution to the g tensor not only increases the average of the g -tensor distribution, it also changes the relative magnitudes of the principal g values. Without orbital contribution, two principal g values are approximately equal and smaller than two, while the third principal g value is close to 2. If the orbital contribution is large, all three principal g values are different and, on average, symmetrically positioned around two.

Petta and Ralph have measured distributions of g factors (i.e., the square root of the G_{zz} element of the g -tensor) for small particles of different metals and found that distributions, if normalized to the average, were in very good agreement with the random matrix theory of Ref. 11. The average of the distribution, however, was up to a factor 10 smaller than the theoretical prediction (30) with a reasonable estimate for the parameter η .¹⁰ A similar discrepancy between a experimental and theoretical estimates was reported in a different context by Marcus *et al.*²⁰ for the magnetic field scale for fluctuations of Coulomb blockade heights in two-dimensional μm -size GaAs/GaAlAs quantum dots (see also Ref. 21). Although the experimental system studied in Refs. 20,21 is quite different from that of Petta and Ralph, the random matrix theories describing the magnetic field dependence of Coulomb blockade peak heights and the orbital contributions to g factors are the same. At present, we do not know of a solution to either puzzle.

One complication in the search for an orbital contribution to the g factors measured in Ref. 7 is that the main effect of the orbital contribution is to change the average of the g -factor distribution only. Since, for strong spin-orbit scattering, the average g factor depends on both the dimensionless spin-orbit coupling λ and the dimensionless orbital contribution η , cf. Eq. (30), it is impossible to characterize what fraction of a measured g factor is

the result of a state's orbital magnetic moment. The recent development of experimental methods to measure the entire g tensor⁸ opens new avenues to investigate the orbital contribution. For weak spin-orbit scattering, the g -tensor distribution depends on the two parameters λ and η in a nontrivial way; even a weak orbital contribution leads to g tensors with, at least, one principal g value larger than two, see, e.g., Fig. 2. Hence, measurement the full g tensors for metal grains with weak spin-orbit scattering, such as large Al grains, eventually doped with a small concentration of Au,⁵ will allow the independent determination of the orbital contribution.

ACKNOWLEDGMENTS

We would like to thank Vinay Ambegaokar, Michael Crawford, Leonid Glazman, Jason Petta, and Dan Ralph for discussions. This work was supported by the Cornell Center for Materials Research under NSF grant no. DMR0079992, by the NSF under grant no. DMR 0086509 and by the Packard foundation.

-
- * Present address: CEA, Service de Physique de l'Etat Condensé, Centre d'Etudes de Saclay, 91191 Gif-sur-Yvette, France.
 - ¹ For a review, see R. C. Ashoori, *Nature* (London) **379**, 413 (1996).
 - ² M. A. Kastner, *Phys. Today* **46** (1), 24 (1993).
 - ³ D.C. Ralph, C.T. Black and M. Tinkham, *Phys. Rev. Lett.* **74** 3241 (1995).
 - ⁴ C. W. J. Beenakker, *Phys. Rev. B* **44** 1646 (1991).
 - ⁵ D. G. Salinas, S. Guéron, D. C. Ralph, C. T. Black, and M. Tinkham, *Phys. Rev. B* **60**, 6137 (1999).
 - ⁶ D. Davidović and M. Tinkham, *Phys. Rev. Lett.* **83**, 1644 (1999); *Phys. Rev. B* **61**, 16359 (2000).
 - ⁷ J. R. Petta and D. C. Ralph, *Phys. Rev. Lett.* **87**, 266801 (2001).
 - ⁸ J. R. Petta and D. C. Ralph, preprint.
 - ⁹ W. P. Halperin, *Rev. Mod. Phys.* **58**, 533 (1986).
 - ¹⁰ K. A. Matveev, L. I. Glazman, and A. I. Larkin, *Phys. Rev. Lett.* **85**, 2789 (2000).
 - ¹¹ P. W. Brouwer, X. Waintal, and B. I. Halperin, *Phys. Rev. Lett.* **85**, 369 (2000).
 - ¹² C. P. Slichter, *Principles of Magnetic Resonance* (Springer, Berlin, 1980).
 - ¹³ A. Pandey and M. L. Mehta, *Commun. Math. Phys.* **87**, 449 (1983).
 - ¹⁴ M. L. Mehta, *Random Matrices* (Academic, New York, 1991).
 - ¹⁵ S. Adam, P. W. Brouwer, J. P. Sethna, X. Waintal *cond-mat/0203002*
 - ¹⁶ C. W. J. Beenakker, *Rev. Mod. Phys.* **69**, 731 (1997).

¹⁷ K. Frahm and J.-L. Pichard, J. Phys. I France **5**, 847 (1995).

¹⁸ The derivation of the numerical coefficient for the ballistic case in Ref. 17 contains a mistake. Following appendix C of Ref. 17, for a ballistic sphere with diffuse boundary scattering one has

$$\begin{aligned}\eta^2 &= \frac{3}{4m^*v_F R^3} \int dt \langle L_z(0) L_z(t) \rangle \\ &= \frac{m^2}{4m^* R^3} \left\langle \frac{|\vec{r}_0 \times \vec{r}_1|^2}{|\vec{r}_0 - \vec{r}_1|} \right\rangle,\end{aligned}$$

where L_z is the orbital angular momentum in the z -direction and the average is taken over all classical trajectories in the sphere. Each trajectory is characterized by the points \vec{r}_i of reflection from the surface; \vec{r}_0 and \vec{r}_1 are the points of reflection immediately before and after time $t = 0$. The joint distribution of \vec{r}_0 and \vec{r}_1 is

$$P(\vec{r}_0, \vec{r}_1) = \frac{3}{16\pi R^5} |\vec{r}_0 - \vec{r}_1|.$$

The factor $|\vec{r}_0 - \vec{r}_1|$, which was not taken into account in Ref. 17, follows from the constraint that \vec{r}_0 and \vec{r}_1 are last and first boundary points before and after time $t = 0$, instead of an arbitrary pair of boundary points along the trajectory. (The flight time between \vec{r}_0 and \vec{r}_1 , and hence the probability to be between \vec{r}_0 and \vec{r}_1 at $t = 0$, is proportional to $|\vec{r}_0 - \vec{r}_1|$.) Performing the double integration over the surface of the sphere then gives Eq. (12).

¹⁹ J. Sone, J. Phys. Soc. Jpn. **42**, 1457 (1977).

²⁰ C. M. Marcus, S. R. Patel, A. G. Huibers, S. M. Cronenwett, M. Switkes, I. H. Chan, R. M. Clarke, J. A. Folk, S. F. Godijn, K. Campman, and A. C. Gossard, *Chaos, Solitons & Fractals* **8**, 1261 (1997).

²¹ S. M. Cronenwett, S. R. Patel, C. M. Marcus, K. Campman, and A. C. Gossard, Phys. Rev. Lett. **79**, 2312 (1997).